

Dissipation and wave-ion interaction in the solar wind: Links between fluid and kinetic theory

E. Marsch

Max-Planck-Institut für Aeronomie, Max-Planck-Str. 2, D-37191 Katlenburg-Lindau, Germany.

Received: 17 June 1999 – Accepted: 12 October 1999

Abstract. In this paper we establish links between turbulence dissipation and wave-particle interactions in the solar corona and wind. Based on quasilinear theory, a set of anisotropic, multi-component fluid equations is derived, which describe the wave-particle interactions of ions with Alfvén waves and ion-cyclotron waves or magnetosonic waves propagating along the mean magnetic field. The associated equations for the wave spectrum and the heating and acceleration of the ions are derived. In fast solar wind streams heavy ions have about equal thermal speeds as the protons and flow faster than them. In order to explain the observed relations, $T_j/T_p \approx m_j/m_p$ and $\mathbf{U}_j - \mathbf{U}_p \approx \mathbf{V}_A$, a numerical fluid-type model is developed, which takes into account the relevant wave-particle interactions. It is shown that left- and right-handed polarized waves propagating away from the Sun parallel to the interplanetary magnetic field can resonantly heat and accelerate minor ions preferentially with respect to the protons in close agreement with the measured characteristics of ion velocity distributions. Finally, some results from a simple analytical model are discussed.

1 Introduction

In high-speed solar wind in interplanetary space the heavy ions are observed to move faster and have higher temperatures than the protons. For reviews of these solar wind phenomena see, e.g., Marsch (1991) and von Steiger et al. (1995). The minor ion species can be considered as test particles, which probe the Alfvén waves and MHD turbulence in the wind and are heated and accelerated by wave-particle interactions. Similarly, the heavy minor ions in coronal holes (Kohl et al., 1997; Cranmer et al., 1999) are important test particles which can supply direct information about the acceleration process and heating mechanism in the coronal hole and interplanetary solar wind. The observed relative abun-

dances of heavy ions, such as O^{6+} or Fe^{8+} , or ions of other minor species coming in various ionization states, range from some 10^{-4} to even smaller numbers (Bame et al., 1970; 1975). Therefore, these ions are not expected to have a significant influence on the evolution of the turbulent wave spectra and the dynamical behaviour of the solar wind itself. Yet, the abundant ${}^4\text{He}^{2+}$ ions can certainly not be considered as test particles. They contribute a non-negligible amount to the total solar wind mass content and thus influence the dynamics of the wind.

Observations of heavy ions have revealed evidence for interplanetary heating ($T_j > 10^6$ K) and preferential acceleration with respect to the protons (Ogilvie et al., 1980; Schmidt et al., 1980; Bochsler et al., 1985; von Steiger et al., 1995; Hefti et al., 1999). In the data there is a clear statistical trend (with the exception of the slow wind) for the temperature ratios T_j/T_p to be proportional to the heavy ion specific masses m_j/m_p . There is evidence for the heavy ions to have about equal thermal speeds. Furthermore, the differential speed, $(\mathbf{U}_j - \mathbf{U}_\alpha)$, of many minor ions with respect to He^{2+} are highly correlated (Schmidt et al., 1980; von Steiger et al., 1995). Since in fast streams Helium ions travel at about the local Alfvén speed ahead of the protons (see, e.g., Marsch et al., 1982b,c, and the comprehensive review on Helium ion observations by Neugebauer, 1981), there is clear evidence that all heavy ions move faster than protons in high-speed wind with $\mathbf{U}_j - \mathbf{U}_p \approx \mathbf{V}_A$.

Recent spectroscopic observations of the widths of Extreme Ultraviolet (EUV) emission lines as obtained from measurements made on the Solar and Heliospheric Observatory (SOHO) indicate that coronal heavy ions, coming in various ionization stages in the corona, are rather hot (Seely et al., 1997; Kohl et al. 1997; Wilhelm et al., 1998), particularly in the polar coronal holes where the electrons are cold, and seem to show some ordering of their kinetic temperatures according to the local gyrofrequencies (Tu et al., 1998). Also, O^{5+} is

found, by means of spectroscopy, to travel much faster than the protons in coronal holes (Cranmer et al., 1999). All these results indicate to wave-particle processes as being responsible for the coronal heating.

For the solar wind case, Hollweg (1974, 1978), Hollweg and Turner (1978), McKenzie et al. (1978), Dusenbery and Hollweg (1981), McKenzie and Marsch (1982), Marsch et al. (1982a), and Isenberg and Hollweg (1983) have calculated and modelled the Alfvén-wave related nonresonant and the ion-cyclotron-wave associated resonant heating and acceleration. These calculations require the knowledge of the wave spectrum and involve complicated integrals over the velocity distributions and spectral densities, which were usually assumed to be given by bi-Maxwellians and power-laws, respectively. Isenberg and Hollweg (1982) also analysed this problem from the multi-ion-fluid point of view. Hu et al. (1997) generalized recently the concept of wave-action conservation to a multi-fluid situation.

In this paper we establish a set of comparatively simple equations, usable in anisotropic multi-fluid equations, in order to describe the cyclotron-resonant interactions of ions with Alfvén and ion-cyclotron or with fast magnetosonic waves in the solar wind and the Sun's corona. These waves are assumed to be fed by a turbulent cascade from MHD-range fluctuations. Many years ago, Marsch et al. (1982a) and Isenberg and Hollweg (1983) have already modelled alpha-particle and heavy-ion temperatures in the near-Sun solar wind at distances beyond $10R_{\odot}$, thereby employing the quasilinear heating rates. Recently Hu et al. (1997), Li et al. (1997) and Czechowski et al. (1998) have done new anisotropic multi-fluid calculations, using ad-hoc mass-proportional heating functions for the heavy ions in the corona and wind. Our paper will provide also some numerical modelling results on heavy ions in the outer corona.

2 Spectral transfer and dissipation of Alfvénic turbulence

The radial and spectral evolution of turbulence in the solar wind has been theoretically described by spectral transfer equations. The first derivation was made by Tu et al. (1984). Subsequently, various other forms of such equations were derived, which are discussed in the review of Tu and Marsch (1995), from which we quote the result:

$$\begin{aligned} \frac{1}{A} \frac{\partial}{\partial r} (A(3V + 2V_A)P(f, r)) - V \frac{\partial}{\partial r} P(f, r) &= (1) \\ &= -2 \frac{\partial}{\partial f} \mathcal{F}(f, r) \end{aligned}$$

Here the radial solar wind speed is V and the Alfvén

speed is V_A . The wave pressure is given by the integral

$$p_A = \frac{1}{8\pi} \int_{f_0}^{f_D(r)} df P(f, r) \quad (2)$$

which extends over the power spectrum $P(f, r)$ in frequency domain limited by the constant lower-bound frequency, f_0 , and spatially varying upper-bound high frequency, $f_D(r)$, which is close to the local proton gyrofrequency and marks the beginning of the dissipation domain. The corresponding wave vector may be defined by $k_D = 2\pi f_D/V$. The wave-energy exchange equation, which is essentially the wave action equation (Jacques, 1978), can also be cast in the form

$$V \frac{d}{dr} p_A = Q_A + \frac{1}{A} \frac{d}{dr} (A F_A) \quad (3)$$

Here $F_A = (3V + 2V_A)p_A$ is the Alfvén wave energy flux. The volumetric heating or (cooling, depending on its sign) rate is obtained from integration of (1) over frequency and reads

$$Q_A = \frac{\mathcal{F}(f_D, r)}{4\pi} - (V + V_A) \frac{P(f_D(r), r)}{4\pi} \frac{df_D(r)}{dr} \quad (4)$$

Here $\mathcal{F}(f, r)$ is the cascading flux function, for which various forms have been proposed and discussed (for a review see, e.g., by Tu and Marsch, 1995). It is assumed to be zero at the lower boundary, f_0 . For a Kolmogorov-type cascade in the inertial domain of the turbulence the flux function is given by

$$\mathcal{F}(f, r) = \frac{C_K}{\sqrt{4\pi\rho(r)(V(r) + V_A(r))}} (P(f, r))^{3/2} f^{5/2} \quad (5)$$

with a constant, C_K , being of order unity. The total mass density in the plasma is denoted by ρ . A constant flux, $\mathcal{F} = \varepsilon$, with the dissipation rate ε implies a Kolmogorov power-law spectrum and the scaling $P(f, r) \sim \varepsilon^{2/3} f^{-5/3}$. Generally, the observed spectra cannot be described by a single spectral exponent, α , but reveal a flatter low-frequency regime with $\alpha = 1$, a steeper domain with $\alpha = 5/3$, which is the turbulence regime proper, and an even steeper dissipation regime with $\alpha = 2 - 3$ (see the review of Tu and Marsch, 1995). Therefore, for such bent spectra there will be an energy cascade to the kinetic scales. The associated dissipation rate may be expressed as $\varepsilon(r) = \mathcal{F}(f_D(r), r)$. It is a function of radial distance, r , from the Sun through the flux function and the background fluid parameters of the wind, especially via the dissipation frequency $f_D(r)$.

Marsch et al. (1996) have studied $\varepsilon(r = Vt)$ as a function of time, t , along the Helios spacecraft trajectories and found it to be highly variable with time at a scale of 1 minute (still two orders of magnitude above the proton cyclotron period). The dissipation rate $\varepsilon(t)$ behaves highly erratic in time and shows intermittency and scaling properties indicating a fractal cascade. Therefore,

the dissipation process might be discontinuous or inhomogeneous. How these purely phenomenological properties of solar wind MHD turbulence are related to the kinetic properties of the ions in the wind remains an open question. In the remainder of this paper we shall study the dissipation process from the kinetic point of view accounting for the multi-fluid nature of the wind, which consists of the most abundant protons and α -particles and much-less abundant minor heavy ions.

The second term in equation (4) stems from inhomogeneity and arises because of the dependence of the upper bound, $f_D(r)$, upon radial distance, r , from the Sun. Therefore, an ever increasing fraction of the high-frequency part of the Alfvén-wave spectrum is swept off by being sent to dissipation. The sweeping process has recently been incorporated in models of flows in coronal funnel and hole by Tu and Marsch (1997) and Marsch and Tu (1997) as the major source of coronal heating. Recently, alternative and complementary scenarios for the dissipation of MHD turbulence involving kinetic Alfvén waves have been suggested by Leamon et al. (1998a,b). The following analysis can in principle be readily expanded to include other wave modes as well.

3 Quasilinear theory of magnetic field fluctuations and the dispersion relation

We reiterate here some basic equations of quasilinear theory (QLT). Usually, the wave fields are decomposed in plane waves with frequency ω_k and wave vector k , assumed to be directed here parallel to the background field, $\mathbf{B}_0 = B_0 \mathbf{e}_x$. The Fourier component of the magnetic field is $\delta \tilde{\mathbf{B}}_k$. The spectral energy density of the magnetic field is given by $B_k = \frac{1}{8\pi} |\delta \tilde{\mathbf{B}}_k|^2$ and evolves according to

$$\frac{\partial}{\partial t} B_k = 2\gamma_k B_k \quad (6)$$

which follows from the Fourier decomposition

$$\delta \mathbf{B}(x, t) = \int_{-\infty}^{\infty} dk \delta \tilde{\mathbf{B}}_k e^{ikx} e^{-i \int_0^t dt' z_k(t')} \quad (7)$$

where x is the coordinate along B_0 , and $k > 0$ means parallel and $k < 0$ anti-parallel propagation. The growth rate, γ_k , or damping rate if it is negative, together with the real frequency, ω_k , give the complex frequency, $z_k = \omega_k + i\gamma_k$, whereby one has $\omega_k = -\omega_{-k}$, $\gamma_k = +\gamma_{-k}$, and thus $z_k^* = -z_{-k}$, and also $\delta \tilde{\mathbf{B}}_k^* = \delta \tilde{\mathbf{B}}_{-k}$, since the magnetic field in equation (7) must be real. The magnetic fluctuation energy density can be normalized to the background value such that $\tilde{B}_k = \frac{B_k}{B_0^2/8\pi}$, with $B_k = B_{-k}$ by definition. It is often more adequate to use the Doppler-shifted frequency, $z'_k = z_k - kU_j$, as measured in the species j frame of reference moving with its bulk speed U_j , drifting along \mathbf{B}_0 . In this proper

frame of species j , the velocities are obtained by replacing the inertial frame coordinates as follows: $V_{\perp} \rightarrow w_{\perp}$, $V_{\parallel} \rightarrow V_{\parallel} - U_j = w_{\parallel}$.

The full dispersion equation for parallel propagating left ($-$ sign) and right ($+$ sign) handed circularly-polarized electromagnetic waves in a multi-component plasma reads, e.g. after Dum et al. (1980), as follows:

$$\left(\frac{ck}{z_k}\right)^2 = 1 + \sum_j \left(\frac{\omega_j}{z_k}\right)^2 \hat{\varepsilon}_j^{\pm}(z'_k, k) \quad (8)$$

with the speed of light denoted by c . The following definitions hold: The ion charge is e_j , the mass is m_j , and the plasma frequency is $\omega_j^2 = \frac{4\pi e_j^2 n_j}{m_j}$. The ion gyrofrequency, given by the definition carrying the sign of the charge, reads as follows $\Omega_j = \frac{e_j B}{m_j c}$. The dielectric constant involves the resonance integral over the pitch angle gradient of the distribution function and reads

$$\hat{\varepsilon}_j^{\pm} = 2\pi \int_0^{\infty} dw_{\perp} w_{\perp} \int_{-\infty}^{\infty} dw_{\parallel} \frac{w_{\perp}/2}{w_{\parallel} - w_j^{\pm}} \times \left((w_{\parallel} - \frac{z'_k}{k}) \frac{\partial}{\partial w_{\perp}} - w_{\perp} \frac{\partial}{\partial w_{\parallel}} \right) f_j(w_{\perp}, w_{\parallel}, t) \quad (9)$$

We introduced the quantity $w_j^{\pm} = \frac{z'_k \pm \Omega_j}{k}$, the real part of which is the resonance speed. The distribution function f_j is understood to be normalized to the number density n_j . Solving (8) for a given real k , gives the complex frequency z_k . Usually there are at least as many modes or branches as there are species in the plasma considered (Mann et al., 1997). Expansion of (8) about the real axis allows one to derive the real and imaginary parts of the frequency (for small growth/damp rate) from the formulae

$$(kV_A)^2 = \sum_j \hat{\rho}_j \Omega_j^2 \Re \hat{\varepsilon}_j^{\pm}(\omega'_k, k) \quad (10)$$

$$\gamma_k = \frac{-\sum_j \hat{\rho}_j \Omega_j^2 \Im \hat{\varepsilon}_j^{\pm}(\omega'_k, k)}{\sum_j \hat{\rho}_j \Omega_j^2 \frac{\partial}{\partial \omega_k} (\Re \hat{\varepsilon}_j^{\pm}(\omega'_k, k))} \quad (11)$$

Here the fractional mass density of species j , which is defined as $\hat{\rho}_j = n_j m_j / \sum_{\ell} n_{\ell} m_{\ell}$, has been used. The Alfvén velocity based on the total mass density, $V_A^2 = B_0^2 / (4\pi \rho)$, has been used to normalize properly the phase speed, and terms of order $(\frac{V_A}{c})^2$ have been neglected as being very small. The denominator of (11) is related with the so-called wave energy related with the sloshing motion of the particles in the wave field. The growth rate, γ_k , as obtained from (11), is to be used in (6) for the evolution of the wave spectrum.

4 Heating and acceleration rates as velocity moments

The diffusion equation of QLT describes the evolution of the velocity distribution function $f_j(\mathbf{V})$ in the inertial

frame of reference, in which the particles and waves are propagating. The diffusion equation can be found for example in the papers of Davidson (1972) or Marsch et al. (1982a). We take velocity moments of $\frac{\partial}{\partial t} f_j$ as given by the cited diffusion equation. The zeroth moment expresses the conservation of density, n_j . The first moment gives the bulk acceleration, and the heating rates are defined by the second moments:

$$\frac{\partial}{\partial t} U_j = \int_{-\infty}^{\infty} d^3 w \sum_{+,-} \int_{k_D}^{\infty} dk \hat{B}_k^{\pm} \Im \left\{ \frac{\Omega_j^2 \mathcal{W}_j f_j}{k(w_{\parallel} - w_j^{\pm}(k))} \right\} \quad (12)$$

$$\frac{\partial}{\partial t} V_{j\parallel}^2 = \int_{-\infty}^{\infty} d^3 w \sum_{+,-} \int_{k_D}^{\infty} dk \hat{B}_k^{\pm} \Im \left\{ \frac{\Omega_j^2 2w_{\parallel} \mathcal{W}_j f_j}{k(w_{\parallel} - w_j^{\pm}(k))} \right\} \quad (13)$$

$$\begin{aligned} \frac{\partial}{\partial t} V_{j\perp}^2 &= \int_{-\infty}^{\infty} d^3 w \sum_{+,-} \int_{k_D}^{\infty} dk \hat{B}_k^{\pm} \\ &\times \Im \left\{ \frac{\Omega_j^2 \left(\frac{z_k^{\pm}}{k} - w_{\parallel} - U_j \right) \mathcal{W}_j f_j}{k(w_{\parallel} - w_j^{\pm}(k))} \right\} \end{aligned} \quad (14)$$

where the pitch-angle gradient of f_j (\mathcal{W}_j has the dimension of a speed) has been abbreviated as

$$\mathcal{W}_j f_j = \left(-\frac{w_{\perp}^2}{2} \frac{\partial}{\partial w_{\parallel}} + \frac{z_k'}{k} - w_{\parallel} \right) f_j(\mathbf{w}) \quad (15)$$

To calculate the rates, one must know the VDF and the spectrum. From a strict theoretical point of view, assuming a given f_j and \hat{B}_k^{\pm} is not a good approach and not self-consistent, since the spectra and VDFs are expected to evolve within a linear growth time, given by $\frac{1}{\gamma_k}$. Yet, this assumption has been made in most of the applications to the solar corona and wind. By summing up equations (12, 13, 14) we obtain the total rate of change of the thermal and kinetic energy for the particles of species j . This relation can be further summed up over all particle species and, by using the dispersion relation (8), further modified to obtain the total energy conservation law within QLT for a multi-component plasma (see Davidson, 1972). By taking the limit $(V_A/c)^2 \rightarrow 0$, the conservation law for the total energy density, E , may be written in the form:

$$\sum_j \frac{\rho_j}{2} (V_{j\parallel}^2 + 2V_{j\perp}^2 + U_j^2) + \sum_{+,-} \int_{k_D}^{\infty} dk \frac{(\delta \tilde{\mathbf{B}}_k^{\pm})^2}{8\pi} = E \quad (16)$$

The summation extends over positive k s only, from the dissipation vector k_D to larger values, and may include waves with left- and right-hand polarizations. This is indicated by the \pm summation exponent or index. The mean thermal speed parallel and perpendicular to the field are defined by the second moments, $V_{j\parallel}^2 = \langle w_{\parallel}^2 \rangle_j$ and $V_{j\perp}^2 = \langle \frac{w_{\perp}^2}{2} \rangle_j$, where the brackets stand for the full velocity space integration and the index j refers to the respective VDF. Note that $\frac{\partial V}{\partial t} = 0$, because the

waves carried by the plasma cannot set the whole plasma in motion, but only generate relative ion motion. Here $V = \sum_j \hat{\rho}_j U_j$. Remember that $\hat{\rho}_j = \rho_j/\rho$ is the fractional mass density of species j . Therefore, the acceleration in (12) is the differential ion acceleration with respect to the ion center of mass frame defined by V .

The rates are mathematically entirely equivalent to the ones based on the dielectric functions as given in Marsch et al. (1982a). However, note the different emphasis here, where the full character of the velocity moments is retained, and the waves appear through the wave spectrum and the particles via their VDF, $f_j(\mathbf{w})$, which are to be evaluated in principle by the equations of QLT. All three rates depend on the imaginary part, which is a Lorentzian of width γ_k and can be considered as the wave-absorption coefficient. It reads:

$$\Im \left\{ \frac{1}{k(w_{\parallel} - w_j^{\pm})} \right\} = \frac{\gamma_k}{(\omega_k \pm \Omega_j - kw_{\parallel} - kU_j)^2 + \gamma_k^2} \quad (17)$$

The case of resonant wave-particle interactions corresponds to weak growth or small damping, i.e. to the limit $\gamma_k \rightarrow 0$. Equation (17) can then be rewritten as a delta function. A resonant relaxation time can be generally defined as

$$\frac{1}{\tau_j^{\pm}(w_{\parallel})} = \Omega_j^2 \frac{\pi}{2} \int_{k_D}^{\infty} dk \hat{B}_k^{\pm} \delta(\omega_k \pm \Omega_j - kw_{\parallel} - kU_j) \quad (18)$$

At this point the phase velocity is required explicitly. We will use for all ions the phase velocity, V_{ph} , of Alfvén waves propagating along the magnetic field in a multi-ion plasma. This velocity can also be obtained directly from the multi-fluid equations (Isenberg and Hollweg, 1982, 1983). For a recent derivation within the context of Alfvén-wave minor-ion interactions see the paper of McKenzie (1994). We start below from our general dispersion relation (8). The expansion for large resonant speeds of the normalized dielectric constant, in the limit $\gamma_k \rightarrow 0$ in which $z_k' \rightarrow \omega_k'$ holds, yields the result

$$V_{ph} = V \pm \left\{ V_A^2 - \sum_j \hat{\rho}_j \left(V_{j\parallel}^2 - V_{j\perp}^2 + \Delta U_j^2 \right) \right\}^{1/2} \quad (19)$$

This is the phase velocity of an Alfvén wave in a differentially drifting multi-ion plasma in the inertial frame. The ion differential speed is $\Delta U_j = U_j - V$, with which each species moves relative to the center of mass frame. The factor in the brackets is the generalized firehose correction. We consider only propagation away from the Sun, implying that $V_{ph} > 0$. The k -integration in (18) can now be performed and yields

$$\frac{1}{\tau_j^{\pm}(w_{\parallel})} = |\Omega_j| \frac{\pi}{2} |k_j^{\pm}| \hat{B}_{k_j^{\pm}}^{\pm} \Theta(k_j^{\pm} - k_D) \quad (20)$$

The step function takes care that only positive wave vectors larger than k_D are considered. Here the resonance wave vector is denoted by $k_j^{\pm} = \frac{\pm \Omega_j}{w_{\parallel} + U_j - V_{ph}}$.

With all these definitions we can finally write the wave-particle transport terms as

$$\frac{\partial}{\partial t} U_j = \sum_{+,-} \int_{-\infty}^{\infty} d^3 w \frac{1}{\tau_j^{\pm}(w_{\parallel})} \mathcal{V}_j f_j \quad (21)$$

$$\frac{\partial}{\partial t} V_{j\parallel}^2 = \sum_{+,-} \int_{-\infty}^{\infty} d^3 w \frac{2w_{\parallel}}{\tau_j^{\pm}(w_{\parallel})} \mathcal{V}_j f_j \quad (22)$$

$$\frac{\partial}{\partial t} V_{j\perp}^2 = \sum_{+,-} \int_{-\infty}^{\infty} d^3 w \frac{(V_{ph} - w_{\parallel} - U_j)}{\tau_j^{\pm}(w_{\parallel})} \mathcal{V}_j f_j \quad (23)$$

$$\mathcal{V}_j f_j = \left(-\frac{w_{\perp}^2}{2} \frac{\partial}{\partial w_{\parallel}} + V_{ph} - w_{\parallel} - U_j \right) f_j(w_{\perp}, w_{\parallel}) \quad (24)$$

where the integration is carried out over the full velocity space. Given a wave spectrum, the relaxation time after (18) or (20) can be calculated and assumed to be represented by its Taylor expansion. Then the above integrals can be performed, which after a partial integration, only involves the calculation of the moments of the VDF and does not require the functional form of $f_j(\mathbf{w})$ explicitly.

5 Relaxation time for a power-law spectrum

In interplanetary space magnetic field fluctuations often obey simple power laws (for a review see, e.g., Tu and Marsch, 1995) with a spectral index, α , which ranges observationally between 1 and 2. Let us assume, therefore, that the spectrum of LHP and RHP waves (see also Goldstein et al., 1994) obeys

$$\hat{B}_k^{\pm} = \hat{B}_{k_0}^{\pm} \left(\frac{k}{k_0} \right)^{-\alpha} \quad (25)$$

Here k_0 is a free reference wave vector, for which the proton inertial length, $k_0 = \Omega_p/V_A$, is a good choice. In the resonant limit and for non-dispersive waves, we obtain from (20) the time scale

$$\frac{1}{\tau_j^{\pm}(w_{\parallel})} = \Omega_p \hat{B}_{k_0}^{\pm} k_0 \left| \frac{\Omega_j}{\Omega_p} \right|^{(2-\alpha)} \left| \frac{V_A}{w_{\parallel} + U_j - V_{ph}} \right|^{(1-\alpha)} \times \pi \Theta(\pm w_{Rj}^{\pm}(k_D) \mp w_{\parallel}) \Theta(\pm w_{\parallel} \mp (V_{ph} - U_j)) \quad (26)$$

We recall that $\hat{B}_{k_0}^{\pm} k_0 \sim (\delta B^{\pm}/B_0)^2$, is equal to the average relative fluctuation amplitude in the dissipation domain. We used $\omega_k = V_{ph} k$ in equations (26). The resonant speed is denoted as

$$w_{Rj}^{\pm} = \frac{\omega_k - kU_j \pm \Omega_j}{k} \quad (27)$$

Note that this speed is negative or positive for the LHP or RHP waves propagating away from the Sun. Here Θ is the step function defined as $\Theta(x) = 1$ for $x > 0$ and $\Theta(x) = 0$ for $x \leq 0$. We may define the typical inverse relaxation time for a thermal particle as the anomalous

wave-particle collision frequency, $\frac{1}{\tau_j^{\pm}(\pm V_{j\parallel})}$, and take this in front of the k -integrals of equations (21, 22, 23). Then the remaining velocity space integration is easily carried out, yielding the simple relaxation rate model for the rate functions as described in Marsch (1998). More precise heating and acceleration rates can then be obtained by carrying the Taylor expansion to higher orders. Note, however, that the $\Theta(x)$ functions limit the velocity space integration to a smaller domain than that extending from $+\infty$ to $-\infty$, and therefore the moments are not complete. If the plasma beta, $\beta_j = (\frac{V_{j\parallel}}{V_A})^2$ is much smaller than unity, which is the case in the solar corona, then the missing parts of the moments are negligibly small.

6 Resonant acceleration and heating rates for a drifting bi-Maxwellian

Since we consider only field-aligned wave propagation here, relating to ion-cyclotron and parallel fast-mode waves, we need to consider those degrees of freedom of single-particle motion which couple strongly to those waves. Observationally, as found in interplanetary space (Marsch et al, 1982a,b,c) the corresponding features in the ion velocity distribution functions are a core temperature anisotropy and a secondary proton or heavy ion component, i.e. an ion beam streaming along \mathbf{B}_0 at a speed of 1-1.5 times the local Alfvén speed. These features are modelled by a VDF which is composed of one (or several) relatively drifting bi-Maxwellian, which is given by

$$f_j(\mathbf{V}) = \frac{(2\pi)^{-3/2}}{V_{j\parallel} V_{j\perp}^2} \exp \left(-\frac{(V_{\parallel} - U_j)^2}{2k_B T_{j\parallel}} - \frac{(V_{\perp})^2}{2k_B T_{j\perp}} \right) \quad (28)$$

With this VDF the heating and acceleration rates can easily be calculated from equations (18, 12, 13, 14). We restrict ourselves to waves (either right-handed, plus sign, or left-handed, minus sign) which propagate away from the solar surface into interplanetary space. The corresponding normalized spectra are denoted by the symbol \hat{B}_k^{\pm} . The rates are:

$$\frac{\partial}{\partial t} U_j = \sum_{+,-} \int_{k_D}^{\infty} dk \hat{B}_k^{\pm} \left(\frac{\Omega_j}{k} \right)^2 k \mathcal{R}_j^{\pm}(k) \quad (29)$$

$$\frac{\partial}{\partial t} V_{j\parallel}^2 = \sum_{+,-} \int_{k_D}^{\infty} dk \hat{B}_k^{\pm} \left(\frac{\Omega_j}{k} \right)^2 (2k w_{Rj}^{\pm}) \mathcal{R}_j^{\pm}(k) \quad (30)$$

$$\frac{\partial}{\partial t} V_{j\perp}^2 = \sum_{+,-} \int_{k_D}^{\infty} dk \hat{B}_k^{\pm} \left(\frac{\Omega_j}{k} \right)^2 (\mp \Omega_j) \mathcal{R}_j^{\pm}(k) \quad (31)$$

Here we introduced the resonance function

$$\mathcal{R}_j^{\pm}(k) = \pi^2 \int_0^{\infty} dw_{\perp} w_{\perp} \left(-\frac{w_{\perp}^2}{2} \frac{\partial}{\partial w_{\parallel}} \mp \frac{\Omega_j}{k} \right) f_j|_{w_{Rj}^{\pm}} \quad (32)$$

This function is essentially equal to the imaginary part of the dielectric constant (see e.g. Marsch, 1982a), evaluated for small γ_k at the cyclotron resonance. $\mathcal{R}_j^\pm(k)$ is proportional to the number of resonant particles and depends on the pitch-angle gradient of $f_j(\mathbf{w})$ at the resonance. For the model VDF of a drifting bi-Maxwellian (32) can be evaluated analytically and reads

$$\mathcal{R}_j^\pm(k) = \sqrt{\frac{\pi}{2}} \exp\left(-\frac{1}{2}(\xi_j^\pm)^2\right) \left(\xi_j^\pm \frac{T_{j\perp}}{T_{j\parallel}} \mp \frac{\Omega_j}{kV_{j\parallel}} \right) \quad (33)$$

with the normalized real part of the resonant speed $\xi_j^\pm = \frac{w_{Rj}^\pm}{V_{j\parallel}}$. Once the spectrum is known the heating and acceleration rates can be evaluated in dependence of the wave spectrum. Often a simple power law form is assumed, such as in the early solar wind studies by Isenberg and Hollweg (1983) or recently by Cranmer et al. (1999) for coronal hole heating. Marsch et al. (1982a) used the quasilinear equation (6) to calculate the spectrum self-consistently. This will also be done in the subsequent section on minor ions in the solar wind.

7 Resonant wave heating and acceleration of heavy ions

7.1 An anisotropic fluid model including wave-particle interactions

The main idea of the model is that preferential acceleration and heating of solar wind minor ions can be achieved via resonant interaction with ion-cyclotron waves (Hollweg and Turner, 1978; Hollweg, 1981; Dusenbery and Hollweg, 1981; and McKenzie and Marsch, 1982) and also with magnetosonic waves (Barnes and Hung, 1973; Marsch et al., 1982a). Dusenbery and Hollweg (1981) did a comprehensive parameter study on the heating and acceleration of heavy ions by left-handed polarized waves for model wave power spectra prescribed according to observations (Behannon, 1976; Denskat and Neubauer, 1982). They assumed drifting bi-Maxwellians for the particle VDFs and found encouraging agreement of their calculations with the observed ion characteristics $T_j/T_p \geq m_j/m_p$ and $U_j > U_p$. Their ideas were further advanced by Marsch et al. (1982a) in a self-consistent fluid-type model, in which the radial evolution of wave spectra was calculated by taking local wave growth or damping into account within the framework of quasilinear theory as described in section 3 and section 6.

We only quote here the stationary equations of motion for the minor ions for simple spherical geometry, where the distance from the Sun is denoted by r . The continuity equation reads

$$\frac{d}{dr}(r^2 \rho_j U_j) = 0 \quad (34)$$

In the momentum equation gravity and the electric field, stemming from the electron pressure gradient, are small (since we assume $T_e \ll T_j$, and our integration starts beyond $20 R_\odot$) and therefore neglected. Then we have for spherical symmetry the set:

$$\left(1 - \frac{V_{j\parallel}^2}{U_j^2}\right) U_j \frac{d}{dr} U_j - \frac{2V_{j\perp}^2}{r} + \frac{d}{dr} V_{j\parallel}^2 = \frac{\partial}{\partial t} U_j \quad (35)$$

The two energy equations, here in terms of the perpendicular and parallel thermal speeds squared, are

$$U_j \left(\frac{d}{dr} V_{j\perp}^2 + \frac{2V_{j\perp}^2}{r} \right) = \frac{\partial}{\partial t} V_{j\perp}^2 \quad (36)$$

$$U_j \frac{d}{dr} V_{j\parallel}^2 + 2V_{j\parallel}^2 \frac{d}{dr} U_j = \frac{\partial}{\partial t} V_{j\parallel}^2 \quad (37)$$

The right-hand sides are the wave-particle interactions terms derived in section 6. These terms are nonlinear functions of the three moments, $U_j, V_{j\parallel}, V_{j\perp}$ and functionals of the wave spectrum, which in turn evolves according to (6), and the growth rate is determined by (11), in which the model distribution function (28) must be used, to close the whole set of equations consistently. Apparently, even when assuming a rigid bi-Maxwellian model VDF, the resulting set of equation is highly nonlinear. It evolves essentially on two spatial scales, the wave length ($\lambda_A = V_A/\Omega_p$) and the solar radius, R_\odot , as the typical fluid scale in the outer corona and wind. Other technical details of the model can be found in the paper of Marsch et al. (1982a).

The model equations comprise the standard double-adiabatic fluid equations (35, 36, 37) but also include energy (temperature) and momentum (differential speed) transfer rates, which are obtained as integrals over the quasi-linear diffusion operator with form-invariant bi-Maxwellian model distributions as given by equations (29, 30, 31). These equations have been integrated numerically. The solar wind speed is defined by $V(r) = \sum_j n_j m_j U_j$. The center of mass speed $V(r)$ cannot be changed by the waves, because their total momentum is negligible.

The inclusion of cyclotron resonance with right-handed polarized waves in the model proved to be very important (Landau damping was already considered by Barnes and Hung, 1973). Not only because these waves are emitted from the solar corona as well as their left-handed counterparts (Behannon, 1976; Goldstein et al., 1994), but also because they provide a limiting mechanism for the differential velocity $U_j - U_p$. They become increasingly more important when the tails of the minor ion distributions move into resonance with these waves. The prominent role of the fast mode in regulating the ion differential speed has long been recognized (Montgomery et al., 1976; Gary et al., 1976; see also the review by Schwartz, 1980). In our model, the nearly non-dispersive magnetosonic waves actually lead to a

'trapping' of the bulk velocity at about the wave phase speed, an effect which explains naturally the observed close correlation of $U_\alpha - U_p$ with V_A and the radial decrease in the He^{2+} differential speed as observed by Helios (Marsch et al., 1982b,c) between 0.3 and 1 AU. This trapping readily follows from the equations (47-49) in the paper by Marsch (1998), which indicate that acceleration and heating ceases when the particles surf the waves.

Self-consistency of the model calculations appears to be of major importance. Namely, if one speaks about ion-cyclotron wave heating and acceleration of minor ions, one has simultaneously to consider the drastic perpendicular heating or parallel cooling caused by these waves in the proton distribution. This heating leads to an erosion of the original wave power spectrum in the frequency range corresponding to proton resonant speeds of a few thermal speeds. The eroded power then is not available anymore for affecting the heavy ions. Therefore, the evolution of the power spectrum is inextricably linked with the evolution of all the parameters, that characterize the energy and momentum state of solar wind and coronal ions (see also the recent paper by Tu and Marsch, 1999).

Finally, it is necessary to emphasize the importance of the inhomogeneity of the expanding solar wind. An Alfvén wave originating in the corona with a frequency ω much less than the local gyrofrequency there, conserves its frequency propagating in the inertial frame away from the Sun and thus becomes gradually an ion-cyclotron wave, which will at larger heliocentric distances where $\omega \approx \Omega_p$ be damped and deliver its energy and momentum to the ions. The frequency sweeping mechanism is modelled by the second term of equation (4). In the context of recent solar-wind modelling this effect has been used to heat the protons (Tu and Marsch, 1997; Marsch and Tu, 1997).

7.2 Illustrative numerical results and discussion

This section presents some numerical results for a spherical geometry of the outer corona and solar wind, which have been obtained by integrating the model equations (34, 35, 36, 37) (Marsch et al., 1982a) for $^{16}\text{O}^{6+}$ and $^{56}\text{Fe}^{8+}$ ions under various boundary conditions at $20 R_\odot$ and for different initial moments $T_{j\parallel}, T_{j\perp}, \Delta U_j = U_j - V$, characterizing the drifting bi-Maxwellian distribution functions in the solar wind reference frame. We have not tried to integrate through the region of the critical sonic point but start in the near-Sun solar wind. Hu et al. (1999) have recently integrated multi-fluid model equations (but without temperature anisotropy and without inclusion of right-hand waves) through the critical point. In the present model the broad-band waves are "injected" at $20 R_\odot$ and are assumed to propagate away from the Sun parallel to the interplanetary magnetic field. For the abundances we have taken n_{O}/n_p

= 0.001 and $n_{\text{Fe}}/n_p = 0.0001$ (see Bame et al., 1975). In the calculations the assumption of initial thermal equilibrium was made, i.e., $U_j = 0, T_{j\parallel} = T_{j\perp} = T_{p\parallel}$ at $z = 20$, where $z = R/R_\odot$ denotes the normalized heliocentric distance. R_\odot was used as a typical scale length for the fluid equations, where the Alfvén length ($\lambda_A = V_A/\Omega_p$) defines a lower limit for the typical scale length of the wave-particle interaction terms. The ratio R_\odot/λ_A has been put equal to 10^4 at $z = 20$. The injected wave spectrum \mathcal{B}_ω^\pm obeys a power law in frequency for both degrees of polarization with $\mathcal{B}_\omega^\pm = \mathcal{B}_{\Omega_p}^\pm (\omega/\Omega_p)^{-\alpha}$ and $\alpha = 1.5$, in accord with the observations (Behannon, 1976; Denskat and Neubauer, 1982; Tu and Marsch, 1995). The wave intensity at Ω_p was initially fixed at one percent of the ambient field energy density, with $\Omega_p \mathcal{B}_{\Omega_p}^\pm = 0.01 B_0^2/8\pi$. As far as the initial values are concerned and the problems involved in the choice of appropriate numbers for the wave energy density, see the discussion in the paper by Marsch et al. (1982a).

Figure 1 shows ion thermal speeds and relative speed of O^{6+} ions $\Delta U_{\text{O}} = U_{\text{O}} - U_p$ in units of V_A versus normalized heliocentric distance from the Sun. The proton relative speed, ΔU_p , is not shown here because it is negligibly small due to the very low heavy ion abundance, which means that the protons determine the center of mass speed, V . Note that the initial phase is characterized by strong cooling of protons parallel and heating of oxygen ions perpendicular to the magnetic field accompanied by a marked preferential acceleration of O^{6+} . After a few hundred λ_A the proton wave interaction saturates at an anisotropy of about $T_{p\perp}/T_{p\parallel} \simeq 1.4$, in qualitative accord with proton observations in fast wind at 0.3 AU (Marsch et al., 1982b). Also, the oxygen ions show the typical signature of cyclotron heating with $T_{\text{O}\perp}/T_{\text{O}\parallel} \simeq 2.0$. From about $z = 21$ on, the wave particle interaction becomes weaker than it was initially, but O^{6+} is still considerably accelerated because at negative resonant velocities in the sunward tails of their distributions the interaction still continues, leading to a slight increase in ΔU_{O} .

Inspection of Figure 1 shows that between $z = 23$ and $z = 24$ a different situation appears. The O^{6+} ions move now increasingly into resonance with the so far undamped right-hand polarized waves. This resonant interaction leads to strong acceleration, marked perpendicular cooling and pronounced parallel heating. Finally, the anisotropy is even reversed with $T_{\text{O}\perp}/T_{\text{O}\parallel} \simeq 0.9$, and the O^{6+} ions are 'trapped' at about the Alfvén speed, which represents a limiting value for ΔU_{O} . In contrast the protons are not significantly affected by the fast waves but still maintain the signature of the initial perpendicular heating. Qualitatively, these results resemble our previous (Marsch et al., 1982a) calculations for He^{2+} , the main difference being that presently, due to the low abundance of O^{6+} , the center of mass frame is virtually identical with the proton frame. The evolution of the wave power spectra for Figure 1 is not

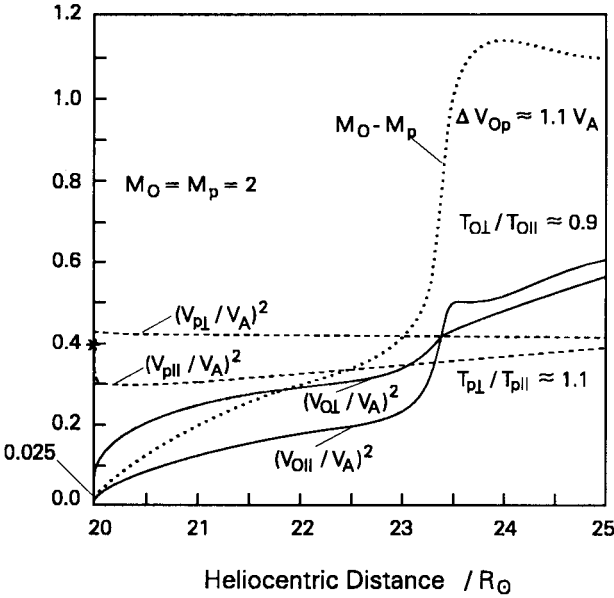


Fig. 1. Hydrogen and oxygen ion thermal speeds squared and oxygen relative speed ΔU_O normalized to the local Alfvén speed (virtually equal to $M_O - M_p$) are shown versus heliocentric distance in units of solar radii. The initial values, $\Delta U_O = \Delta U_p = 0$ and $T_O = T_p$, correspond to thermal equilibrium. Note the strong proton cooling parallel to the magnetic field (lower broken curve delineates $(V_{p\parallel}/V_A)^2$). Oxygen ions are accelerated by magnetosonic waves up to about $\Delta U_O \simeq V_A$ (dotted line). They finally ($z = 24 - 25$) show the signature typical of fast-mode wave heating $T_{O\parallel} > T_{O\perp}$ (continuous lines).

shown here. The radial variation of the spectra resembles qualitatively the one found for the proton - He^{2+} plasma (Marsch et al., 1982a).

It can clearly be seen in Figure 1 that O^{6+} is preferentially heated with respect to the protons. The initial values of $V_{p\parallel}^2 = V_{p\perp}^2 = 0.4 V_A^2$ and $V_{O\parallel}^2 = V_{O\perp}^2 = 0.025 V_A^2$ correspond to equal temperatures at $z = 20$. After the wave-particle interaction has saturated the parallel thermal speeds are about equal at $z = 23.5$ in good agreement with the observations at 1 AU (Ogilvie et al., 1980; Schmidt et al., 1980; von Steiger et al., 1995; Hefti et al., 1999). It should be noted that evidence for fast mode heating ($T_{\alpha\parallel} > T_{\alpha\perp}$) has been found in the He^{2+} distributions in high-speed solar wind (Marsch et al., 1982c) and also the frequent occurrence of a high energy tail or heat flux in α -particle distributions (Marsch et al., 1982c; Ogilvie et al., 1980). Unfortunately, there are still no detailed observations available concerning the temperature anisotropy of heavy ions. If future measurements could also provide the ratio $T_{O\parallel}/T_{O\perp}$ we would expect this anisotropy to be larger than one.

According to equation (33) the number of resonant particles depends exponentially upon Ω_j/Ω_p , which implies a very sensitive discrimination between the various heavy ion species due to the kinematics of the resonance (Hollweg, 1981; McKenzie and Marsch, 1982; Marsch et al., 1982a). The damping or growth rates (11) for the

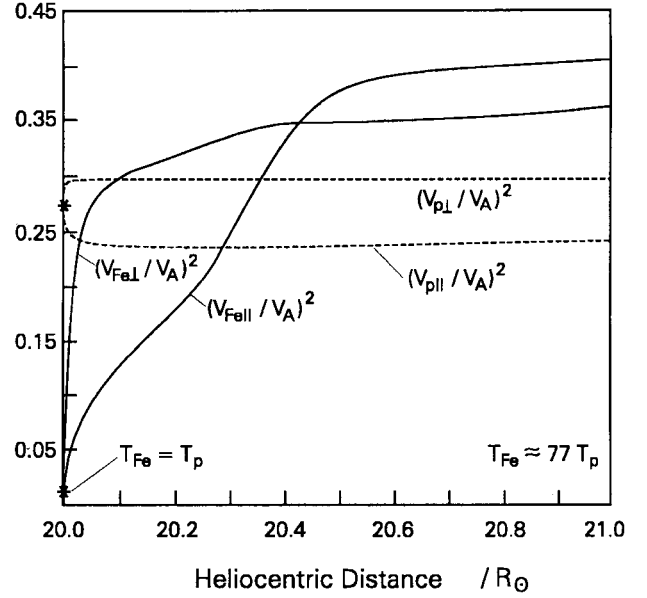


Fig. 2. In a similar format as in Figure 1, the iron (continuous lines) and hydrogen ion (dashed lines) plasma betas, i.e. their speeds squared in units of V_A , are displayed versus radial solar distance. Initial values at $z = 20$ correspond to local thermal equilibrium.

wave spectrum comprises a sum over contributions from all species, which are proportional to their abundance n_j/n_p , respectively. Thus, only protons and He^{2+} (with $n_\alpha/n_p = 0.05$) have a significant influence on the radial evolution of the wave spectra. Concerning the ratio of the gyrofrequencies, Fe^{8+} represents an extreme case, because $\Omega_{\text{Fe}}/\Omega_p = 1/7$ is comparatively small.

In Figure 2 the ion plasma betas (thermal speeds squared in units of the local Alfvén speed) and in Figure 3 the Machnumber (flow speed normalized to the local Alfvén speed) are shown versus normalized heliocentric distance for the heavy Fe^{8+} ions and the protons. Note the similar general course of the curves in Figure 2 compared with those for O^{6+} in Figure 1. But the abscissa only covers $1.0 R_\odot$ in the present case. Obviously, as shown in Figure 3, the initial acceleration of iron by ion-cyclotron waves is much more effective than for O^{6+} shown in Figure 1. The Fe^{8+} ion distribution is drastically heated up perpendicular and somewhat more weakly parallel to the field. After about $0.1 R_\odot$ one obtains $V_{\text{Fe}\perp} \simeq V_{p\perp}$, although the initial values ($T_{\text{Fe}} = T_p$) corresponded to thermal equilibrium. As soon as ΔU_{Fe} exceeds about $0.5 V_A$ (corresponding to $M_{\text{Fe}} \geq 2.5$) the tail of the iron distribution moves into resonance with right-handed polarized waves, which leads to additional acceleration now in connection with strong heating parallel to field. Finally, the typical signature of fast mode heating ($T_{\text{Fe}\parallel} > T_{\text{Fe}\perp}$) appears, and the relative speed ΔU_{Fe} reaches about the Alfvén speed for $M_{\text{Fe}} > 3.1$ beyond $z = 20.8$.

To demonstrate how a variation of the injected wave

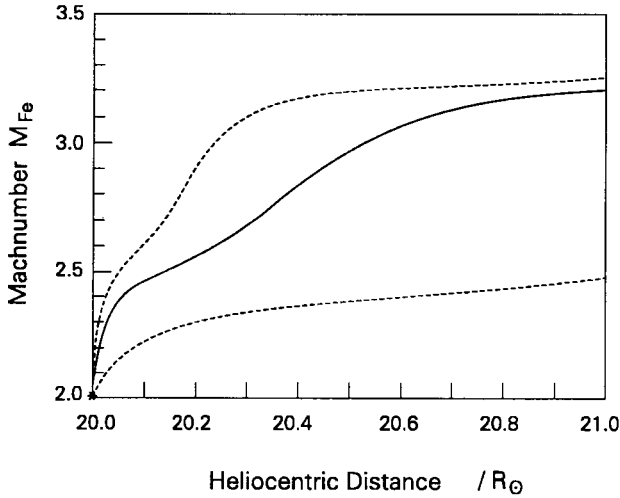


Fig. 3. Mach number of the Fe^{8+} ions displayed versus normalized heliocentric distance. The continuous line pertains to Figure 2 with a normalized wave energy density at the proton gyrofrequency of 0.005, the broken top (bottom) curves to a relative wave energy increased (reduced) to a fluctuation level of 0.01 (0.001).

intensity changes the initial heavy ion acceleration, two additional curves (broken) in Figure 3 are shown. The continuous trace corresponds to $\Omega_p \mathcal{B}_{\Omega_p}^{\pm} = 0.005 (B_0^2/8\pi)$ (pertaining to Figure 2), the top broken curve to 0.01 and the lower one to 0.001. One can see that a change by an order of magnitude in wave intensity drastically reduces the initially achievable acceleration and leads to a larger scale length, which has to be traveled through by a heavy ion, in order to accomplish a significant differential speed with respect to the protons. It should also be noted that the iron Mach number, M_{Fe} , is initially 2.0 and then increases strongly between $z = 20$ and 21. For the lower curve, M_{Fe} reaches a value of about 3.2 (corresponding to $\Delta U_{\text{Fe}} \simeq 1.1V_A$) not before $z = 28$, but then also stays at about this value.

8 Rates for a drifting bi-Maxwellian in relaxation-rate form

In the previous section we have presented numerical solutions of a simple anisotropic fluid model for heavy ions expanding in a monopole-field geometry. We have included wave-ion interactions, whereby the VDF was fixed and the kinetic degrees of freedom restricted to $V_{\parallel}, V_{\perp}, U_j$, but the wave spectrum was calculated self-consistently such as in Marsch et al. (1982a). In contrast to this model, we consider now a homogeneous system and describe the evolution of the moments without requiring the detailed knowledge of the wave spectrum. Rather general evolutionary trends of the moments $V_{\parallel}, V_{\perp}, U_j$ can still be derived that way. The rates (29, 30, 31) can be rewritten in a relaxation-rate form and be analytically integrated under certain sim-

plifying assumptions in order to obtain more insight into the wave-particle interaction processes. For this purpose let us define a normalized spectral average (with $\ll 1 \gg = 1$) of any function $Q(k)$ as follows:

$$\ll Q \gg^{\pm} = \frac{\Omega_j^2}{\nu_j^{\pm}} \sqrt{\frac{\pi}{2}} \int_{k_D}^{\infty} dk \hat{\mathcal{B}}_k^{\pm} \frac{Q(k)}{k V_{j\parallel}} \exp\left(-\frac{1}{2}(\xi_j^{\pm})^2\right) \quad (38)$$

$$\nu_j^{\pm} = \Omega_j^2 \sqrt{\frac{\pi}{2}} \int_{k_D}^{\infty} dk \hat{\mathcal{B}}_k^{\pm} \frac{1}{k V_{j\parallel}} \exp\left(-\frac{1}{2}(\xi_j^{\pm})^2\right) \quad (39)$$

where the average relaxation rate ν_j^{\pm} has been defined. Then the acceleration and heating rates attain the form

$$\begin{aligned} \frac{\partial}{\partial t} U_j &= - \sum_{+,-} \nu_j^{\pm} \left\{ \left(\ll U_j - \frac{\omega_k}{k} \gg^{\pm} \right) \left(\frac{V_{j\perp}}{V_{j\parallel}} \right)^2 \right. \\ &\quad \left. \pm \ll \frac{\Omega_j}{k} \gg^{\pm} \left(1 - \left(\frac{V_{j\perp}}{V_{j\parallel}} \right)^2 \right) \right\} \quad (40) \end{aligned}$$

$$\begin{aligned} \frac{\partial}{\partial t} V_{j\perp}^2 &= \sum_{+,-} \nu_j^{\pm} \left\{ \pm \ll \left(U_j - \frac{\omega_k}{k} \right) \frac{\Omega_j}{k} \gg^{\pm} \left(\frac{V_{j\perp}}{V_{j\parallel}} \right)^2 \right. \\ &\quad \left. + \ll \left(\frac{\Omega_j}{k} \right)^2 \gg^{\pm} \left(1 - \left(\frac{V_{j\perp}}{V_{j\parallel}} \right)^2 \right) \right\} \quad (41) \end{aligned}$$

$$\begin{aligned} \frac{1}{2} \frac{\partial}{\partial t} V_{j\parallel}^2 &= \sum_{+,-} \nu_j^{\pm} \left\{ \ll \left(U_j - \frac{\omega_k}{k} \right)^2 \gg^{\pm} \left(\frac{V_{j\perp}}{V_{j\parallel}} \right)^2 \right. \\ &\quad \pm \ll \left(U_j - \frac{\omega_k}{k} \right) \frac{\Omega_j}{k} \gg^{\pm} \left(1 - 2 \left(\frac{V_{j\perp}}{V_{j\parallel}} \right)^2 \right) \\ &\quad \left. - \ll \left(\frac{\Omega_j}{k} \right)^2 \gg^{\pm} \left(1 - \left(\frac{V_{j\perp}}{V_{j\parallel}} \right)^2 \right) \right\} \quad (42) \end{aligned}$$

We have just formally rewritten the equations (29 – 31) here. The strongest variability is expected for the rate ν_j^{\pm} , since it contains the spectrum, whereas the other averages, due to normalization, are presumably much less variable than ν_j^{\pm} , and may be considered to be about constant. In the following we only consider the simple case of an isotropic electron-proton plasma including dispersion. Under these assumptions equations (8, 9) yield the dispersive phase speed:

$$\frac{\omega'_k}{k} = V_{ph} - V = V_A \sqrt{1 \pm \frac{\omega'_k}{\Omega_p}} \quad (43)$$

The frequency in the ion center of mass frame is denoted by $\omega'_k = \omega - kV$. More refined estimates of V_p can be obtained from the full dispersion equation (8). We shall make the approximation $\omega'_k \cong \Omega_j$, and evaluate the wave phase velocity at that frequency. With $\omega'_k \approx \Omega_j$ one

finds the typical wave vector $\kappa_j^\pm = \frac{\Omega_j}{V_A \sqrt{1 \pm \Omega_j/\Omega_p}}$. With this vector the specific phase speed

$$V_{Aj}^\pm = V_A \sqrt{1 \pm \Omega_j/\Omega_p} \quad (44)$$

can be defined, and the normalized relaxation rate be cast in the form

$$\frac{\nu_j^\pm}{\Omega_j} = \sqrt{\frac{\pi}{2}} \left(\frac{\delta B^\pm}{B_0} \right)^2 \exp\left(\frac{-(V_{Aj}^\pm(1 \pm 1) - \Delta U_j)^2}{2V_{j\parallel}^2} \right) \frac{V_{Aj}^\pm}{V_{j\parallel}} \quad (45)$$

which only involves the integrated spectrum or average wave amplitude in the dissipation domain. We recall that $\int_{k_D}^\infty dk \hat{B}_k^\pm = (\delta B^\pm/B_0)^2$.

9 Solution of simplified model equations

With the approximations made in the previous section we have obtained a closed set of rate equations. In this way one can obtain valuable insights in the evolution of the coupled moments as a function of time in a homogeneous system. The three moments equations can compactly be written by introduction of the plasma betas and Mach number for each species j . The plasma beta is defined by $\beta_{j\parallel,\perp} = \left(\frac{V_{j\parallel,\perp}}{V_{Aj}} \right)^2$ and the Mach number in the solar wind (ion center of mass) frame by $M_j^\pm = \frac{U_j - V}{V_{Aj}^\pm}$. We further define the variable $\delta_j^\pm = 1 \pm 1 \mp M_j^\pm$, which also appears in the exponential function of equation (45). It is convenient to measure time in units of the relaxation time defined through $t_j^\pm = \frac{1}{\nu_j^\pm} \frac{T_{j\parallel}}{T_{j\perp}}$, where the temperature ratio has been included for mathematical simplicity of the subsequent equations. We abbreviate the dimensionless time derivative of any variable x as $t_j^\pm \frac{d}{dt} x = \dot{x}$. For the sake of simplicity, let us consider now either LHP or RHP waves only. Then there is no \pm sum and the three coupled equations (40, 41, 42) read

$$\dot{\delta}_j^\pm = -(\delta_j^\pm - \beta_{j\parallel}^\pm/\beta_{j\perp}^\pm) \quad (46)$$

$$\frac{1}{2}\dot{\beta}_{j\parallel}^\pm = \delta_j^\pm(\delta_j^\pm - \beta_{j\parallel}^\pm/\beta_{j\perp}^\pm) \quad (47)$$

$$\dot{\beta}_{j\perp}^\pm = -(\delta_j^\pm - \beta_{j\parallel}^\pm/\beta_{j\perp}^\pm) \quad (48)$$

This set of equations looks formally alike for the two wave types. Yet, note that $\delta_j^+ = 2 - M_j^+$ and $\delta_j^- = M_j^-$, which is the Machnumber itself. For the sake of lucidity we omit in what follows all the indices and consider only LHP waves. Then the above set reduces to the coupled three nonlinear equations:

$$\dot{M} = -(M - \beta_{\parallel}/\beta_{\perp}) \quad (49)$$

$$\frac{1}{2}\dot{\beta}_{\parallel} = M(M - \beta_{\parallel}/\beta_{\perp}) \quad (50)$$

$$\dot{\beta}_{\perp} = -(M - \beta_{\parallel}/\beta_{\perp}) \quad (51)$$

The dots denote derivatives in terms of the dimensionless time variable, $s(t)$, given by $s = \int_0^t \frac{1}{t_j^\pm(t')} dt'$, which is the history in relaxation times and similar to the optical depth in radiation transfer. We take the initial conditions $M_0 = 0, \beta_{\parallel} = \beta_{\parallel 0}, \beta_{\perp} = \beta_{\perp 0}$ and omit the subscripts below to ease the notation. It can immediately be seen from the above nonlinear equations that there exist two integrals, $\beta_{\parallel} + M^2 = \text{const}$ and $\beta_{\perp} - M = \text{const}$. Exploiting these relations, one obtains finally for the Mach-number a single nonlinear differential equation, which reads

$$\dot{M} = -2 \frac{(M - M_1)(M - M_2)}{M - 2(M_1 + M_2)} \quad (52)$$

The solution $M(s)$ starts with a positive slope, given by the initial temperature ratio at time zero. This slope reads $\dot{M}|_{s=0} = \frac{\beta_{\parallel}}{\beta_{\perp}} > 0$. From equation (52) it is clear that $M(s)$ has two stationary solutions: $M = M_1$ and $M = M_2$. For a positive initial slope, $M(s)$ will approach M_1 asymptotically. The equation (52) has the characteristic zeroes

$$M_{1,2} = -\frac{\beta_{\perp}}{4} \pm \sqrt{\left(\frac{\beta_{\perp}}{4}\right)^2 + \frac{\beta_{\parallel}}{2}} \quad (53)$$

and a singularity at $2(M_1 + M_2) = -\beta_{\perp}$, and is readily integrated. The formal solution is given by the implicit equation

$$\exp(2(M_1 - M_2)s) = \left| \frac{M - M_1}{M_1} \right|^{(M_1 + 2M_2)} \times \left| \frac{M - M_2}{M_2} \right|^{-(2M_1 + M_2)} \quad (54)$$

The most transparent case is the one with $\beta_{\perp} = \sqrt{\beta_{\parallel}}$, which implies that $2M_1 + M_2 = 0$. Then one finds the simple exponential asymptotic solution

$$M(s) = \frac{\beta_{\perp}}{2} (1 - e^{-2s}) \quad (55)$$

The final state at the dimensionless time s being infinity has the parameters

$$M(\infty) = \frac{1}{2}\beta_{\perp}; \quad \beta_{\parallel}(\infty) = \frac{3}{4}\beta_{\parallel}; \quad \beta_{\perp}(\infty) = \frac{3}{2}\beta_{\perp} \quad (56)$$

which yields an asymptotic anisotropy of $\frac{T_{\parallel}}{T_{\perp}} = \frac{1}{2}$, if the initial state was isotropic and had a beta of unity. The final differential speed, $\Delta U = \frac{1}{2}V_{\parallel}$, is half of the initial thermal speed. That means the wave acceleration is weak in a low-beta plasma. If one starts with a high-beta cigar-type distribution, with $\beta_{\perp} = 2$ and $\beta_{\parallel} = 4$, then $M(\infty) = 1$ and $T_{\parallel}(\infty) = T_{\perp}(\infty)$, which means that the particles ride the waves with an isotropic velocity distribution. Note that these trends and numbers are consistent with the numerical results of the model in section 7 for the phase, where LHP waves dominate

the wave-particle interactions. The general asymptotic anisotropy is

$$\frac{T_{\parallel}(\infty)}{T_{\perp}(\infty)} = \frac{4\beta_{\parallel} - \beta_{\perp}^2 + \beta_{\perp}\sqrt{\beta_{\perp}^2 + 8\beta_{\parallel}}}{6\beta_{\perp} + 2\sqrt{\beta_{\perp}^2 + 8\beta_{\parallel}}} \quad (57)$$

which depends on both initial plasma betas. What comes out quite clearly from these calculations is that it is impossible, when starting from near isotropy, to reach a large anisotropy with $T_{\perp} \gg T_{\parallel}$. That is prevented by the structure of the equations (40, 41, 42), which results in turn from the structure of the original rate equations (29, 30, 31) and anisotropy-dependent resonance function (32, 33). This function depends explicitly on the pitch-angle gradient, and thus the limitation of the anisotropy reflects the effective pitch-angle scattering of the particles by the waves, as it is described by the diffusion equation (see, e.g., Marsch, 1998) from which the rates were derived.

10 Conclusions

The detailed rate equations derived here in the sections 4 and 6 and the related general ones described previously in sections 6 and 7 of Marsch (1998) can be incorporated in multi-fluid models of the solar corona and wind, thus complementing and expanding the models put forward recently for the corona by Hu et al. (1999), Li et al. (1997), and Czechowski et al. (1998), or years ago for the solar wind by Isenberg and Hollweg (1983). In modelling the behaviour of minor ions in the solar wind, there has in the past been a debate (see e.g. Marsch et al., 1982a; Isenberg and Hollweg, 1983) about whether dispersive waves are able to produce sizable differential speeds and what the influence of dispersion is in this process. A detailed study should be carried out in the future to evaluate quantitatively the effects of wave dispersion and damping on the differential ion speed and temperature a given species might attain in the solar corona and wind.

The influence of resonant wave-particle interactions on the dynamics of minor heavy ions in the solar wind has been investigated. The model described here has previously been proved successful in describing basic characteristics of observed proton and α -particle distributions (Marsch et al., 1982a,b,c). It has been shown that ion-cyclotron waves propagating away from the Sun along \mathbf{B}_0 are capable of accelerating heavy ions through the proton bulk speed. These waves also preferentially heat the minor ions perpendicular to the field and raise in this way their average temperature, until T_j amounts finally to a considerable multiple, more than A_j times, of the proton temperature.

The inhomogeneity of the expanding wind (note that V_A and Ω_p decrease with increasing solar distance) has the effect that the fastest heavy ions in the tails of the

distributions move into increasingly stronger resonance with right-handed polarized magnetosonic waves. These waves now further accelerate the heavy ions until their differential speed is about V_A . Also, they can preferentially heat the particles parallel to the field to the effect that finally their temperature anisotropy shows the signature of fast wave heating $T_{j\parallel} > T_{j\perp}$ and that $V_{j\parallel} \approx V_{p\parallel}$ is accomplished. This near equalization of thermal speeds is one of the most striking observed characteristics of heavy solar wind ions at 1 AU (Schmidt et al., 1980; Ogilvie et al., 1980; von Steiger et al., 1995).

Self-consistency has been shown to be crucial in order to describe the radial evolution of wave spectra, because proton damping or wave excitation can lead to a dramatic reshaping of the originally injected wave spectrum or even a complete erosion of the wave power (Tu and Marsch, 1999). Therefore, typical relaxation times for the dynamic equilibrium between heavy ions and waves can certainly be orders of magnitudes larger than estimated on the base of rigid wave spectra. On the other hand, evaluation of the wave spectra requires an integration on the kinetic scales of the ions, which is not what one wants for a fluid description of the expanding wind in the corona. As a compromise, one may rely on fixed wave spectra, such as Cranmer et al. (1999) and Hu et al. (1999) did again recently in their coronal hole models, yet one must be aware of the limitations of such an approach. Certainly, further improvements in the models must be made.

Acknowledgement. Helpful discussions with C.Y. Tu and comments by J.F. McKenzie are gratefully acknowledged.

References

- Bame, S. J., J. R. Asbridge, A. J. Hundhausen, and M. D. Montgomery, 1970, Solar wind ions: $^{56}\text{Fe}^{+8}$ to $^{56}\text{Fe}^{+12}$, $^{28}\text{Si}^{+7}$, $^{28}\text{Si}^{+8}$, $^{28}\text{Si}^{+9}$, and $^{16}\text{O}^{+6}$, *J. Geophys. Res.* 75, 6360
- Bame, S. J., J. R. Asbridge, W. C. Feldman, M. D. Montgomery, and P. D. Kearney, 1975, Solar wind heavy ion abundances, *Solar Phys.* 43, 463
- Barnes, A., and R. J. Hung, 1973, On the kinetic temperature of He in the solar wind, *Cosmic Electrodynamics* 3, 416.
- Behannon, K. W., 1976, Observations of the Interplanetary Magnetic Field between 0.41 and 1 AU by the Mariner 10 spacecraft, GSFC X Document, 692-76-2
- Bochsler, P., Geiss, J., Joos, R., 1985, Kinetic temperatures of heavy ions in the solar wind, *J. Geophys. Res.* 90, 10779-10789
- Cranmer, S.R., Kohl, J.L., Noci, G., et al., 1999, An empirical model of a polar coronal hole at solar minimum, *Astrophys. J.* 511, 481
- Czechowski, A., Ratkiewicz, R., McKenzie, J.F., Axford, W.I., 1998, Heating and acceleration of minor ions in the solar wind, *Astron. Astrophys.* 335, 303-308
- Davidson, R.C., 1972, *Methods in Nonlinear Plasma Theory*, Academic, New York
- Denskat, K. U., and F. M. Neubauer, 1982, Statistical Properties of Low-Frequency Magnetic Field Fluctuations in the Solar Wind from 0.29 to 1 AU during Solar Minimum Conditions: Helios-1 and Helios-2, *J. Geophys. Res.* 87, 2215

- Dusenbery, P.B., Hollweg, J.V., 1981, Ion-cyclotron heating and acceleration of solar wind minor ions, *J. Geophys. Res.* 86, 153-164
- Dum, C.T., Marsch, E., Pilipp, W.G., 1980, Determination of wave growth from measured distribution functions and transport theory, *J. Plasma Phys.* 23, 91-113
- Gary, S. P., M. D. Montgomery, W. C. Feldman and D. W. Forslund, 1976, Proton temperature anisotropy instabilities in the solar wind, *J. Geophys. Res.* 81, 1241
- Goldstein, M. Roberts, D.A., Fitch, C.A., 1994, Properties of the fluctuating magnetic helicity in the inertial and dissipation ranges of solar wind turbulence, *J. Geophys. Res.* 99, 11519-11538
- Hefti, S., Grünwaldt, H., Ipavich, F.M., Bochsler, P., Hovestadt, D., Aellig, M.R., Hilchenbach, M., Galvin, A.B., Geiss, J., Gliem, F., Gloeckler, G., Klecker, B., Marsch, E., Möbius, E., Neugebauer, M., Wurz, P., 1999, Kinetic properties of solar wind minor ions and protons measured with SOHO/CELIAS, *J. Geophys. Res.*, in press
- Hollweg, J.V., Turner, J.M., 1978, Acceleration of solar wind He^{++} : 3. Effects of resonant and nonresonant interactions with transverse waves, *J. Geophys. Res.* 83, 97-113
- Hollweg, J. V., 1981, Helium and Heavy Ions, in "Solar Wind 4", H. Rosenbauer, ed., MPAE-W-100-81-31, Report of the Max-Planck-Institut für Aeronomie, F. R. Germany
- Hu, Y.-Q., Esser, R., Habbal, S.R., 1997, A fast solar wind model with anisotropic temperature, *J. Geophys. Res.* 102, 14661-14676
- Hu, Y.-Q., Habbal, S.R., 1999, Resonant acceleration and heating of solar wind ions by dispersive ion cyclotron waves, *J. Geophys. Res.*, in press
- Isenberg, P.A., Hollweg, J.V., 1982, Finite amplitude Alfvén waves in a multi-ion plasma: Propagation, acceleration and heating, *J. Geophys. Res.* 87, 5023-5029
- Isenberg, P.A., Hollweg, J.V., 1983, On the preferential acceleration and heating of solar wind heavy ions, *J. Geophys. Res.* 88, 3923-3935
- Jacques, S.A., 1978, Solar wind models with Alfvén waves, *Astrophys. J.* 226, 632-649
- Kohl, J.L., Noci, G., Antonucci, E., et al., 1997, First results from the SOHO UltraViolet Coronagraph Spectrometer, *Solar Phys.* 175, 613-644
- Leamon, R.J., Matthaeus, W.H., Smith, C.W., Wong, H.K., 1998a, Contribution of cyclotron-resonant damping to kinetic dissipation of interplanetary turbulence, *Astrophys. J. Lett.* 507, L181-L184
- Leamon, R.J., Smith, C.W., Ness, N.F., W.H. Matthaeus, Wong, H.K., 1998b, Dissipation range dynamics: kinetic Alfvén waves and the importance of β_e , *J. Geophys. Res.* 103, 4775-4787
- Li, X., Esser, R., Habbal, S.R., Hu, Y.-Q., 1997, Influence of heavy ions on the high-speed solar wind, *J. Geophys. Res.* 102, 17419-17432
- Mann, G., Hackenberg, P., Marsch, E., 1997, Linear mode analysis in multi-ion plasmas, *J. Plasma Phys.* 58, 205-221
- Marsch, E., 1991, Kinetic physics of the solar wind, in *Physics of the Inner Heliosphere*, R. Schwenn and E. Marsch, Eds., Springer Verlag, Heidelberg, Germany, Vol. II, pp. 45-133
- Marsch, E., 1998, Closure of multi-fluid and kinetic equations for cyclotron-resonant interactions of solar wind ions with Alfvén waves, *Nonlinear Proc. in Geophys.* 5, 111-120
- Marsch, E., Goertz, C.K., Richter, K., 1982a, Wave heating and acceleration of solar wind ions by cyclotron resonance, *J. Geophys. Res.* 87, 5030-5044
- Marsch, E., Mühlhäuser, K.H., Schwenn, R., Rosenbauer, H., Pilipp, W., Neubauer, F., 1982b, Solar wind protons: Three-dimensional velocity distributions and derived plasma parameters measured between 0.3 and 1 AU, *J. Geophys. Res.* 87, 52-72
- Marsch, E., Mühlhäuser, K.H., Rosenbauer, H., Schwenn, R., Neubauer, F., 1982c, Solar wind helium ions: Observations of the Helios solar probes between 0.3 and 1 AU, *J. Geophys. Res.* 87, 35-51
- Marsch, E., Tu, C.-Y., Rosenbauer, H., 1996, Multifractal scaling of the kinetic energy flux in solar wind turbulence, *Ann. Geophysicae.* 14, 259-269
- Marsch, E., Tu, C.-Y., 1997, Solar wind and chromospheric network, *Solar Phys.* 176, 87-106
- McKenzie, J.F., Ip, W.-H., Axford, W.I., 1978, Anomalous acceleration of minor ions in the solar wind, *Nature* 274, 350-351
- McKenzie, J.F., Marsch, E., 1982, Resonant wave acceleration of minor ions in the solar wind, *Astrophys. Space Sci.* 81, 295-314
- McKenzie, J.F., 1994, Interaction between Alfvén waves and a multicomponent plasma with differential ion streaming, *J. Geophys. Res.* 99, 4193-4200
- Montgomery, M. D., S. P. Gary, W. C. Feldman, and D. W. Forslund, 1976, Electromagnetic instabilities driven by unequal proton beams in the solar wind, *J. Geophys. Res.* 81, 2743
- Neugebauer, M., 1981, Observations of solar wind Helium, *Fundamentals of Cosmic Physics* 7, 131
- Ogilvie, K. W., P. Bochsler, J. Geiss, and M. A. Coplan, 1980, Observations of the Velocity Distribution of Solar Wind Ions, *J. Geophys. Res.* 85, 6069
- Seely, J.F., Feldman, U., Schühle, U., Wilhelm, K., Curdt, W., Lemaire, P., 1997, Turbulent velocities and ion temperatures in the solar corona obtained from SUMER line widths, *Astrophys. J.* 484, L87-L90
- Schmidt, W.K.H., H. Rosenbauer, E. G. Shelley, and J. Geiss, 1980, On temperature and speed of He^{2+} and O^{6+} ions in the solar wind, *Geophys. Res. Lett.* 7, 697
- Schwartz, S., 1980, Plasma Instabilities in the Solar Wind: A Theoretical Review, *Rev. Geophys. Space Phys.* 18, 313
- Tu, C.Y., Pu, Z.Y., Wei, F.-S., 1984, The power spectrum of interplanetary Alfvénic fluctuations: Derivation of the governing equation and its solution, *J. Geophys. Res.* 89, 9695
- Tu, C.Y., Marsch, E., 1995, MHD structures, waves and turbulence in the solar wind: Observations and theories *Space Science Rev.* 73, 1-210
- Tu, C.-Y., Marsch, E., 1997, A two-fluid model for heating of the solar corona and acceleration of the solar wind by high-frequency Alfvén waves, *Solar Phys.* 171, 363-391
- Tu, C.Y., Marsch, E., Wilhelm, K., Curdt, W., 1998, Ion temperatures in a solar polar coronal hole observed by SUMER on SOHO, *Astrophys. J.* 500, 475-482
- Tu, C.-Y., Marsch, E., 1999, Study of the heating mechanism of solar wind ions in coronal holes, *Solar Wind 9*, AIP Conference Proceedings, 471, 373-376
- von Steiger, R., Geiss, J., Gloeckler, G., Galvin, A.B., 1995, Kinetic properties of heavy ions in the solar wind from SWICS/Ulysses, *Space Science Rev.* 72, 71-76
- Wilhelm, K., Marsch, E., Dwivedi, B.N., Hassler, D.M., Lemaire, P., Gabriel, A., Huber, M.C.E., 1998, The solar corona above polar coronal holes as seen by SUMER on SOHO, *Astrophys. J.* 500, 1023-1038